A Control Lyapunov Function-Based Quadratic Program for the Cable-Driven Boat Motion Simulator

Joonyoung Jang
Mechanical and Aerospace Engineering Department
University of California, San Diego
San Diego, USA
j7jang@eng.ucsd.edu

Muhan Zhao

Mechanical and Aerospace Engineering Department

University of California, San Diego

San Diego, USA

muz021@eng.ucsd.edu

Thomas Bewley
Mechanical and Aerospace Engineering Department
University of California, San Diego
San Diego, USA
bewley@eng.ucsd.edu

Abstract—This paper proposes a Control Lyapunov Function-based Quadratic Program (CLF-QP) approach for controlling a cable-driven parallel robot. We consider the cable-driven boat motion simulator to verify that the CLF-QP approach controls platform motions following the desired trajectories and optimizes cable tensions in the desired boundaries. A simulation model with a moving platform and 8 cables was used for testing CLF-QP controller. 6 degrees of freedom (DOF) periodic and mathematical ship model motion were applied to the simulation. The results show that the normalized root mean square errors(NRMSE) of motion tracking were less than 7%, and cable tensions were bounded in the range set by a user without constraint violations in optimization processes.

Keywords-Cable-driven parallel robot, Control Lyapunov Function, Tension optimization, Quadratic program

I. INTRODUCTION

Cable-driven parallel robots (CDPRs) consist of a moving platform and multiple cables. Such systems can be classified as tensegrity structures that are lightweights, but robust to high payloads due to the use of cables reducing weight and inertia [1-3]. CDPRs maneuver a tensegrity structure from the initial equilibrium state to desired states satisfying the control input constraints such as cable tensions limits. Since cables only can pull a platform but cannot push it, cables must be in tension to apply forces on a platform. However, there are not many studies on dynamic controls with tension optimizations, while earlier works primarily focused on kinematics, accurate motion control, and applications of CDPRs [4-6]. The controllers of CDPRs have to deal with both controlling platform motions and maintaining cable tensions in the desired range. If cable tensions are too high, structures or cables can be damaged, and if tensions are too low, cables cannot put forces on a platform properly. CDPRs that have more cables than their DOF is defined as underdetermined CDPRs. As the underdetermined CDPRs hold many feasible tension solutions at each equilibrium

state [7], cable tensions can be optimized in the desired boundaries.

For solving control problems of CDPRs, the Proportional Integral Derivative (PID) and Linear Quadratic Regulator (LQR) controllers for CDPRs were suggested, and research showed the performances of these controllers [8-10]. However, these studies focused on motion controls, and cable tension optimization needs to be considered in control processes.

In our previous research about the control and tension optimization of the cable-driven boat motion simulator, the Linear Matrix Inequality (LMI) based controller was suggested for controlling the cable-driven boat motion simulator [11]. We developed a simulation model based upon the tensegrity system's kinematics and dynamics. The simulation results demonstrated that the LMI controller controls moving platform motions accurately, and cable tensions were optimized in the desired boundaries by the standard deviation method. However, the linearization process of tensegrity system dynamics and cable tension optimization algorithms were too complex. Thus, the computational efforts were too heavy to control an experimental hardware model.

We propose a Control Lyapunov Function-based Quadratic Program (CLF-QP) controller design method. The CLF-based approach is the nonlinear controller design method for the closed-loop feedback control system [12]. The CLF controller could be practically used for a wide range of applications, including systems with fast sample rates [13].

By choosing an appropriate CLF that satisfies certain conditions, the optimal input that stabilizes a system can be determined. The existence of a CLF indicates that a system is stabilizable, and the QP method combined with the CLF approach can conserve the performance characterized by a CLF and respect constraints on the inputs assigned by users,

such as tension boundaries [14]. The simulation model of the cable-driven boat motion simulator was used for analyzing the CLF-QP controller. The purpose of the simulator is to replicate 6-DOF boat motions for developing a drone landing control system. A flat-plate rectangular platform is connected to 8 cables and moves following the desired trajectories.

This paper mainly discusses the novel control method for cable-driven parallel robots that control moving platform motions while cable tensions are within the maximum and the minimum tension limits. The optimized system inputs were obtained by leveraging the CLF-QP controller design method. The simulation model test was performed and showed the motion control performances and tension optimization results.

The organization of this paper is as follows. Section II discusses cable-driven parallel robots' kinematics and dynamics. Section III introduces the CLF-based controls and formulates QP to find the optimized control inputs. Section IV demonstrates the simulation results of CLF-QP applications to the cable-driven boat motion simulation model. Finally, we present the conclusion and the future works in Section V.

II. KINEMATICS AND DYNAMICS

The following introduces important properties of cabledriven parallel robots regarding kinematics and dynamics.

A. Kinematics and Static Equilibrium

Fig. 1 is the configuration of the cable-driven boat motion simulator. The global frame O_G is located in the center of the ground, and the body frame O_B is in the middle of the moving platform, where the platform's center of gravity is located. \vec{a} denotes the pulley position vector, $i = \{1, \dots, n\}$ represents the i-th cable and n is the number of cables. $\vec{p} = [x \ y \ z]^T$ is the moving platform position vector in the global frame O_G , and \vec{b} is the cable attachment point vector in the body frame O_B with R, the platform rotation matrix in the global frame O_G . The cable vector \vec{l} can be determined by inverse kinematics equations [15],

$$\vec{l}_i = \vec{a}_i - R\vec{b}_i - \vec{p}, \quad (i = 1, \dots, n).$$

All forces by cable tensions must be equivalent to any external forces and moments applied to the platform to achieve equilibrium. The equilibrium condition of the platform can be written as [16],

$$J\vec{\tau} = \vec{f}$$
,

where J is the structure matrix, $\vec{\tau} = [\tau_1, \dots, \tau_n]^T$ is a cable tension vector, and \vec{f} is a vector that represents the sum of all forces and moments on the platform. Let $\vec{d_i}$ be a

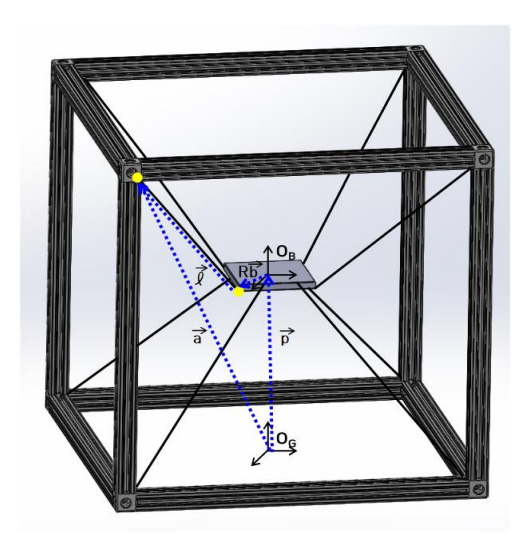


Fig. 1. The cable-driven boat motion simulator configuration. A fl at-plate re ctangular pl atform is connected with 8 cables, and motors adjust cable lengths. Upper and lower cables are cross-connected to the platform for better rotational motions.

unit cable vector that is defined as $\vec{d_i} = \vec{l_i}/||l_i||$, then J can be defined as,

$$J = \begin{bmatrix} \vec{d_1} & \cdots & \vec{d_n} \\ R\vec{b_1} \times \vec{d_1} & \cdots & R\vec{b_n} \times \vec{d_n} \end{bmatrix}.$$

B. Dynamics

Defining the platform state vector $\vec{r} = [x \ y \ z \ \phi \ \theta \ \psi]^T$ and gravitational acceleration vector as $G = \begin{bmatrix} 0 & 0 & q & 0 & 0 \end{bmatrix}^T$ with the platform mass m and the gravitational acceleration q, the dynamic equation of moving a platform can be written as [17],

$$J\vec{\tau} = M\ddot{\vec{r}} + C\dot{\vec{r}} + MG,\tag{1}$$

where M, and C are the platform mass and Coriolis matrices

$$M = \begin{bmatrix} mI_{3\times3} & 0_{3\times3} \\ 0_{3\times3} & I_{g_{3\times3}} \end{bmatrix}, \quad C = \begin{bmatrix} 0_{3\times3} & 0_{3\times3} \\ 0_{3\times3} & I_g + \omega \times I_g \end{bmatrix},$$

with the identity matrix I and the moment of inertia of a platform I_g . $\omega = [\omega_x \ \omega_y \ \omega_z]^T$ denotes the platform angular velocity vector. The term $J\vec{\tau} \in \mathcal{R}^{6 \times 1}$ in (1) represents force and moment vector induced by cable tensions. (1) can be rewritten in the matrix form about the platform state vector

$$\begin{bmatrix} \dot{\vec{r}} \\ \ddot{\vec{r}} \end{bmatrix} = \begin{bmatrix} 0 & I \\ 0 & -M^{-1}C \end{bmatrix} \begin{bmatrix} \vec{r} \\ \dot{\vec{r}} \end{bmatrix} + \begin{bmatrix} 0 \\ M^{-1}(J\vec{\tau} - MG) \end{bmatrix}. \quad (2)$$

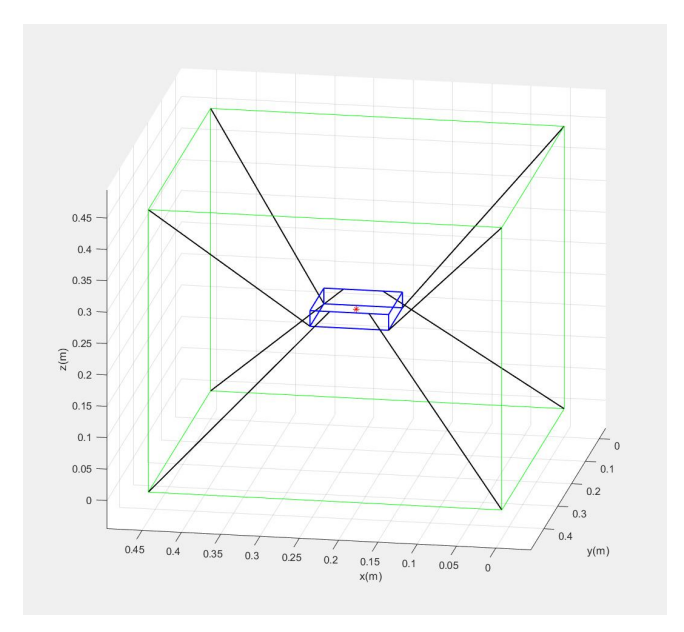


Fig. 2. The simulation model of the cable-driven boat motion simulator. The Green lines are the outer structure, the black lines are cables, the blue lines are the platform, and the red dot is the mass center of the platform.

Considering that cable tension $\vec{\tau}$ as the input of the dynamic model and taking $\vec{\tau}$ out of the matrix, then (2) becomes,

$$\begin{bmatrix} \dot{\vec{r}} \\ \ddot{\vec{r}} \end{bmatrix} = \begin{bmatrix} 0 & I \\ 0 & -M^{-1}C \end{bmatrix} \begin{bmatrix} \vec{r} \\ \dot{\vec{r}} \end{bmatrix} + \begin{bmatrix} 0 \\ -G \end{bmatrix} + \begin{bmatrix} 0 \\ M^{-1}J \end{bmatrix} \vec{\tau}. \quad (3)$$

III. CONTROLS

The controllers of CDPRs require to perform motion control and tension optimization. In this research, the CLF-QP controller is suggested to achieve these goals, and the following describes applying the CLF-QP approach to CDPRs.

A. Control Lyapunov Function

Consider the following dynamic system,

$$\dot{x} = f(x) + g(x)u,\tag{4}$$

where x is the state vector, f(x) and g(x) are continuous functions of x. Let u be the feedback control input that stabilizes the system. Assume that V(x) is a smooth, positive definite function and define $L_fV(x)$, and $L_qV(x)$ as,

$$L_f V(x) = \frac{\delta V}{\delta x} f(x), \quad L_g V(x) = \frac{\delta V}{\delta x} g(x). \tag{5}$$

Then, V(x) that satisfies following inequality,

$$\dot{V}(x) = L_f V(x) + L_g V(x) u < 0, \quad \forall x \neq 0, \tag{6}$$

is called a Control Lyapunov Function (CLF) [18], and it gives a sufficient condition for the stabilizability of systems.

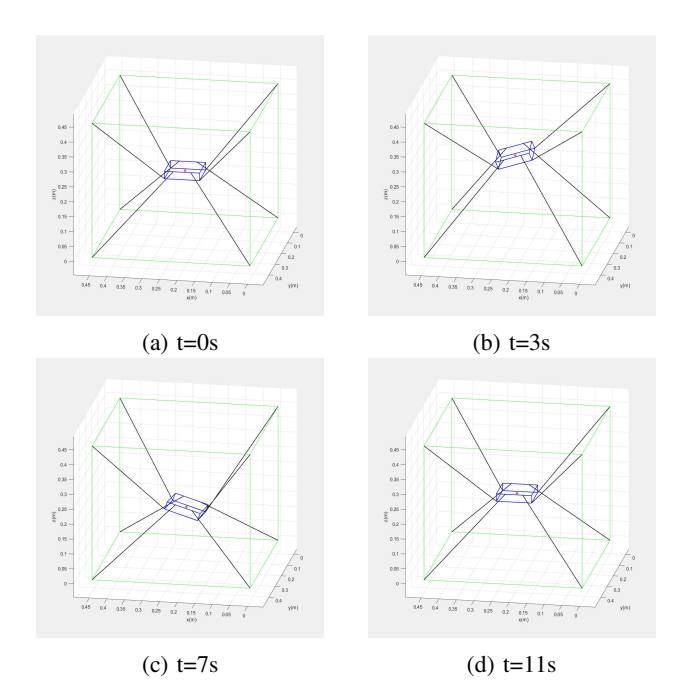


Fig. 3. The platform configurations over time (Periodic).

The existence of CLFs indicates that there exists feedback control u stabilizes the system [19] and the inequality (6) induces that the system is asymptotically stable. However, there is no information about the convergence rate to the equilibrium. To construct the upper bound of V(x) and impose a condition of the minimum rate of decrease in V(x), (6) can be rewritten with an additional term $\lambda V(x)$ [20],

$$\dot{V}(x) = L_f V(x) + L_g V(x) u + \lambda V(x) < 0, \quad \forall x \neq 0,$$
(7)

where λ represents the decay rates of V(x).

B. Application of CLF to CDPR Dynamics

Let x be the state of a moving platform such that, x = $[\vec{r} \ \vec{r}]$, and a control input $u = [\vec{\tau}]$ as a cable tension vector. By the dynamic equation (3) and (4), functions f(x) and g(x) can be defined as,

$$f(x) = \begin{bmatrix} 0 & I \\ 0 & -M^{-1}C \end{bmatrix} \begin{bmatrix} \vec{r} \\ \vec{r} \end{bmatrix} + \begin{bmatrix} 0 \\ -G \end{bmatrix},$$

$$g(x) = \begin{bmatrix} 0 \\ M^{-1}J \end{bmatrix}.$$
(8)

The CLF was chosen as $V(x) = ||x - x_d||_2^2$, where $x_d =$ $[\vec{r}_d \ \ \dot{\vec{r}}_d]$ is the desired platform state. The gradient of V(x)becomes as follows,

$$\frac{\delta V}{\delta x} = 2(x - x_d),$$

and by (5), $L_fV(x)$, and $L_gV(x)$ can be written as,

$$L_f V(x) = 2(x - x_d)^T \left(\begin{bmatrix} 0 & I \\ 0 & -M^{-1}C \end{bmatrix} \begin{bmatrix} \vec{r} \\ \vec{r} \end{bmatrix} + \begin{bmatrix} 0 \\ -G \end{bmatrix} \right),$$

$$L_g V(x) = 2(x - x_d)^T \begin{bmatrix} 0 \\ M^{-1}J \end{bmatrix}.$$

C. CLF-based Quadratic Program

As discussed above, CDPR controllers need to deal with controlling platform positions and maintaining cable tensions while a platform moves. The quadratic program (QP) was implemented as the QP preserves performances expected by CLF and respects the user-defined constraints on the inputs [14] [21]. CLF-QP can be written as a convex optimization problem, and the standard form of CLF-QP is as follows [22],

where \vec{u}_d is the reference input. Define the tension margins as the difference between the current tensions and the maximum or minimum tension limits. Tensions need to be optimized near the mean value of the maximum and the minimum tension limits to maximize tension margins [11]. One can set reference input \vec{u}_d as the mean value of tension limits to maintain tensions close to \vec{u}_d . Also, the optimal cable tensions have to be within tension limits and satisfy the dynamic equation. Since these are hard constraints, there needs a relaxation to the bound on the CLF to avoid conflict on constraints. By adding constraints and relaxation, (9) becomes,

$$\underset{\vec{u},\delta}{\operatorname{argmin}} \quad (\vec{u} - \vec{u}_d)^T (\vec{u} - \vec{u}_d) + p \delta^2$$

$$\operatorname{subject to} \quad L_f V(x) + L_g V(x) + \lambda V(x) \leq \delta$$

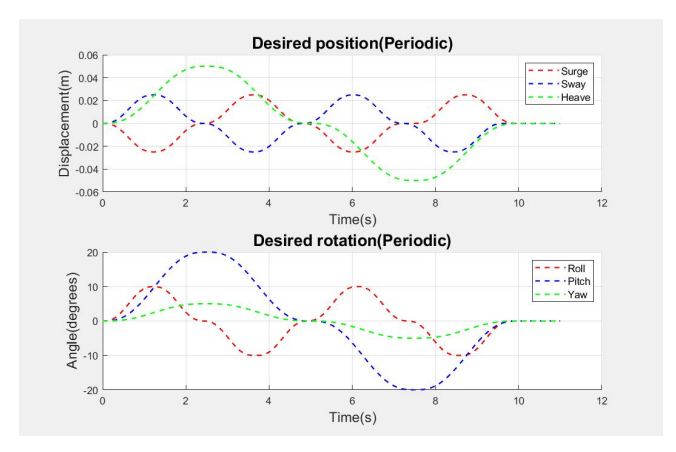
$$\vec{u}_{min} \leq \vec{u} \leq \vec{u}_{max}$$

$$J\vec{u} = M\vec{\vec{r}}_d + C\vec{\vec{r}}_d + MG, \tag{10}$$

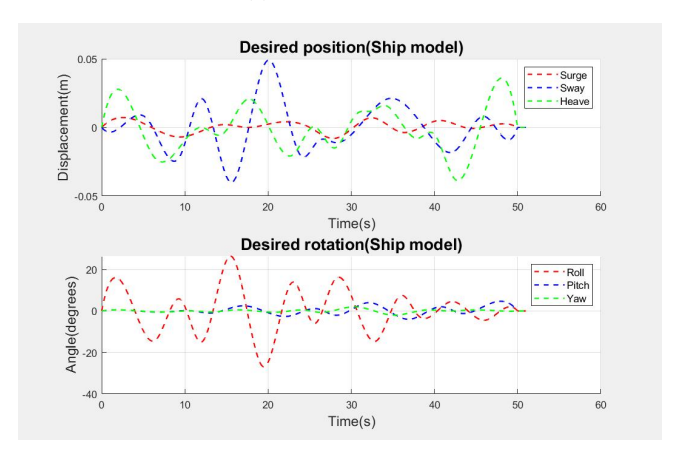
where δ is a positive constant that relaxes CLF constraints, and p is the positive number that represents the penalty of δ . u_{min} and u_{max} are the minimum and the maximum tension limits set by a user. The optimal control input $u = [\vec{\tau}]$ can be directly determined by solving (10). The platform states by cable tensions are calculated from the dynamic equation (1) using the Runge-Kutta method.

IV. RESULTS

In this section, simulation results are discussed to verify the performance of the CLF-QP method. The 6-DOF boat motion simulator model has a moving platform and 8 cables. 2 different desired motions were applied to the simulation: Periodic and mathematical ship model motions.



(a) Periodic motion



(b) Ship model motion

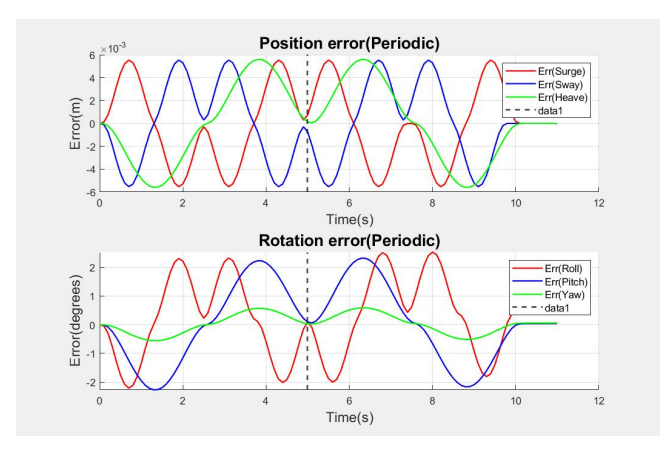
Fig. 4. The desired motions of a platform.

Table I. Desired motion of a platform: Periodic

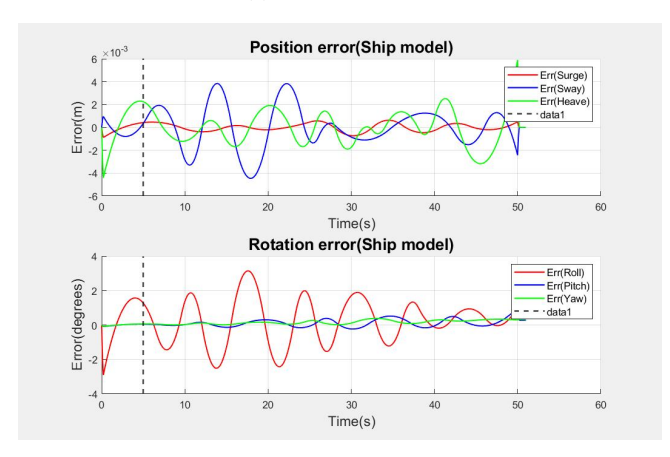
Motion	Range	Period(seconds)
Surge	-0.025 - 0.025 m	5
Sway	-0.025 - 0.025 m	5
Heave	-0.050 - 0.059 m	10
Roll	-10°- 10°	5
Pitch	-20°- 20°	10
Yaw	-5°- 5°	10

A. Model and Simulation Description

The simulation model configuration is shown in Fig. 2, and Fig. 3 is the configuration of the periodic motion simulation test over time. The model's size is equivalently set to the hardware model currently being built in the Coordinated Robotics Lab, University of California, San Diego. The edge of the outer structure is 45cm, and the platform is a 10cm flat rectangular plate. The height of the platform is 2.5cm, and the mass is 0.213kg. The lower cables are connected to the inward point on the top, while the upper cables are to the bottom edges of the platform. Cables are cross-attached to the platform for better rotational motions. Cable mass







(b) Ship model motion

Fig. 5. Motion tracking errors. The black dashed vertical lines are the time t=5 when a drone lands on a platform. Controller constants were set as p = 0.01, and $\lambda = 1$.

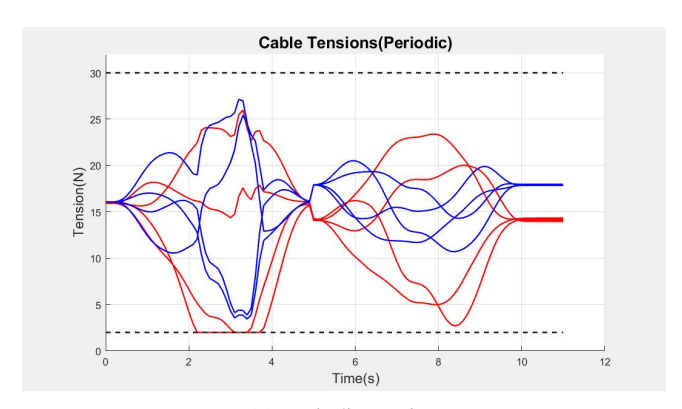
is assumed as negligible, and structures are not deformed by tensions. The cable material is Kevlar which has a high Young's modulus $(76 \times 10^9 N/m^2)$. Thus, cables are assumed as non-stretchable. The maximum and the minimum tension limits are set as 2N and 30N, respectively. The platform moves in 6-DOF motions for 10 seconds (periodic) and 50 seconds (ship model). After the motion, both cases have a 1-second stationary state at the origin. In this simulation scenario, at the time t = 5s, a 1kg mass drone lands on a platform. Hence, the total mass of a platform increases after 5 seconds. The simulation time-step size is 0.1 seconds and for solving optimization uses CVX solver, a MATLAB package for specifying and solving optimization programs [23-24].

B. Simulation Results

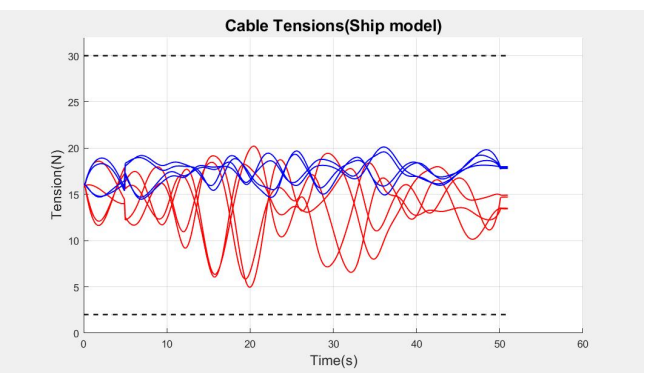
1) Tracking errors: The desired platform motions are shown in Fig. 4. First, the periodic motion was applied to the simulation. The motion details are shown in Fig.

Table II. Motion tracking RMSE, NRMSE

Motion	RMSE(NRMSE): Periodic	RMSE(NRMSE): Ship model
Surge	0.0034m (6.73%)	0.0003m (2.22%)
Sway	0.0034m (6.73%)	0.0018m (1.97%)
Heave	0.0034m (3.39%)	0.0016m (2.07%)
Roll	1.3704° (6.85%)	1.3223° (2.47%)
Pitch	1.3650° (3.41%)	0.2289° (2.70%)
Yaw	0.3387° (3.39%)	0.1941° (4.84%)



(a) Periodic motion

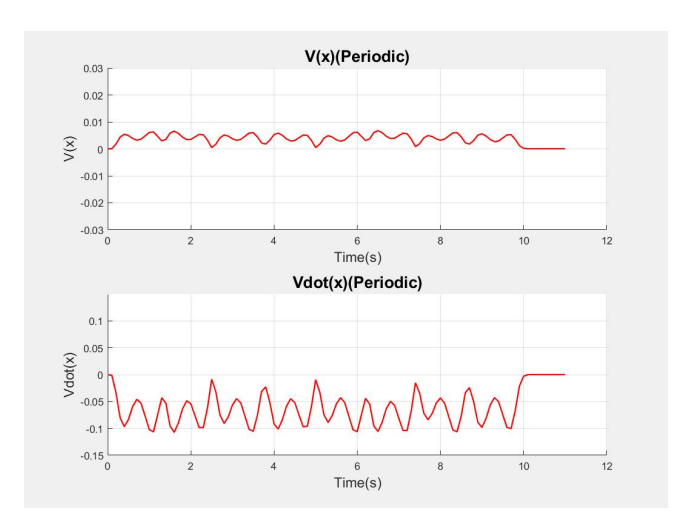


(b) Ship model motion

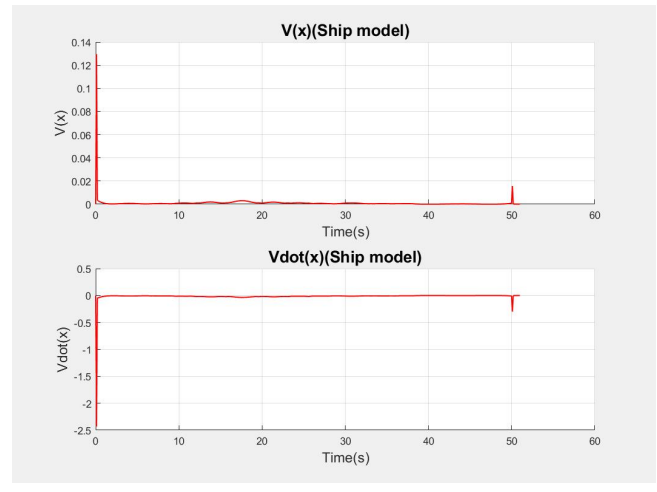
Fig. 6. Cable tensions. The red lines are lower cables, and the blue lines are upper cables. Black dashed lines are the minimum and the maximum tension limits.

4a, and Table I. The translational and rotational motion tracking errors are as seen in Fig. 5a. The position error was $-5.60 \times 10^{-3} \sim 5.60 \times 10^{-3}$ m and the rotation error was $-2.29 \sim 2.23^{\circ}$.

Next, Fig. 4b shows the desired motion obtained by the mathematical ship motion model, the USS navy ship Oliver Hazard Perry Class Frigate at a sea state 6 with 60 degrees of wave direction [25]. Since the simulation model is smaller than the real ship, the system sizes and the amplitudes of motions have to be scaled down [26]. The position (surge, sway, and heave) amplitude was scaled down with 1/100ratio, while the same magnitude of rotation was used. Fig. 5b shows the tracking error of the ship model simulation. The position error was $-4.5 \times 10^{-3} \sim 5.9 \times 10^{-3}$ m and



(a) Periodic motion: V(x) is within the boundary $0 \sim 0.0063$, and V(x) is $-0.1067 \sim 0$.



(b) Ship model motion: V(x) is within the boundary $0 \sim 0.1295$, and $\dot{V}(x)$ is $-2.4343 \sim 0$.

Fig. 7. Control Lyapunov Function V(x), and $\dot{V}(x)$

the rotation error was $-2.91 \sim 3.14^{\circ}$.

The root mean square errors (RMSE) and the percentage of normalized RMSE (NRMSE) for both motions are shown in Table II. The difference between the maximum and minimum values of the desired trajectory was used as a scaler to normalize RMSE. The result demonstrates the CLF-QP tracks the desired motions less than 7% NRMSE, and the platform state was stable after the motion. At the time t=5, a drone landed on a moving platform in the scenario, and 1kg additional mass was added to the platform mass. The RMSE of the tracking error without drone landing was equivalent to Table II, and the CLF-QP controller maintained its performance after a drone landing on the platform.

2) Cable tensions: Fig. 6 shows the cable tension changes while a moving platform is in motions. In both simulation scenarios, cable tensions were optimized without optimization violations. Tensions were within the boundary that was set before running the simulation. In the periodic motion, the lower cable tensions were maintained within $2 \sim 22.978N$, and the upper cable tensions were within $3.446 \sim 27.129N$. At the time between $2 \sim 4$ seconds, two of the lower cables reached the minimum tension limit. However, the controller found tension solutions that did not exceed tension limits and maintained tensions of all cables within the desired tension boundaries. In the ship model motion, the lower cable tensions changed within $4.96 \sim 20.21$, and the upper cable tensions were within $14.48 \sim 20.13N$. In this scenario, cable tensions did not reach tension limits and were sustained within the desired tension boundaries.

3) CLF and stability: As described in §III, if a positive function V(x) satisfies the inequality $\dot{V}(x) < 0$, a system is stable at the equilibrium with the feedback control input.

As seen in Fig. 7, a CLF V(x) was positive while a platform was in motion and eventually converged to zero in both cases. $\dot{V}(x)$, defined as (7), was negative for whole process. This indicates that the system is stable with an optimal input $u = [\vec{\tau}]$ that is calculated by (10).

V. CONCLUSION AND FUTURE WORKS

This study presents a CLF-based QP controller for the cable-driven boat motion simulator. Controllers of cabledriven parallel robots are required to control the motions of the platform and perform cable tension optimization. A simulation model was suggested to test the performance of the controller. 6-DOF periodic motion and ship model motion were used as desired motions. The results illustrate that the CLF-QP controller can be useful to control a platform motion of CDPRs with tension limits set by users. The CLF-QP controller controls a platform motion with small errors and maintains cable tensions in the desired boundaries without optimization violations. The future work focuses on building a hardware model of the cable-driven boat motion simulator with tension sensors to verify simulation results. The size of the simulator will be equivalent to the simulation model, and the larger scale (10x15x5m) simulator is also considered to build in Aerodrome at the University of California, San Diego. The larger scale simulator will be used for developing the drone landing control system. The study of drone landing control system includes the research of the platform pose estimation, and the landing controller drives the drone lands on a platform when the platform rotation is within the drone's capacity.

REFERENCES

[1] R. E. Skelton, R. Adhikari, J. Pinaud, W. Chan and J. W. Helton, An introduction to the mechanics of tensegrity structures, Proceedings of the 40th IEEE Conference on Decision and Control (Cat. No.01CH37228), 2001, pp. 4254-4259, doi: 10.1109/CDC.2001.980861.

- [2] R. Mersi, S. Vali, M. S. haghighi, G. Abbasnejad and M. T. Masouleh, Design and Control of a Suspended Cable-Driven Parallel Robot with Four Cables, 2018 6th RSI International Conference on Robotics and Mechatronics (IcRoM), 2018, pp. 470-475, doi: 10.1109/ICRoM.2018.8657534.
- [3] R. E. Skelton and M. C. Oliveira, Tensegrity systems. Springer, 2009.
- [4] J. Seon, S. Park, S. Y. Ko and J. Park, Cable configuration analysis to increase the rotational range of suspended 6-DOF cable driven parallel robots, 2016 16th International Conference on Control, Automation and Systems (ICCAS), 2016, pp. 1047-1052, doi: 10.1109/ICCAS.2016.7832438.
- [5] P. Gallina, A. Rossi, and R. Williams, Planar Cable-Direct-Driven Robots, Part II: Dynamics and Control. Proceedings of the ASME Design Engineering Technical Conference, 2001, doi: 10.1071/ASEG2001ab148.
- [6] P. Miermeister et al., The CableRobot simulator large scale motion platform based on cable robot technology, 2016 IEEE/RSJ International Conference on Intelligent Robots and Systems (IROS), 2016, pp. 3024-3029, doi: 10.1109/IROS.2016.7759468.
- [7] A. Pott, T. Bruckmann, and L. Mikelsons, Closed-form Force Distribution for Parallel Wire Robots, Fraunhofer IPA, 2009, doi: 10.1007/978-3-642-01947-0-4.
- [8] M. A. Khosravi, and H. D. Taghirad, Robust PID control of fully-constrained cable driven parallel robots, Mechatronics, Volume 24, Issue 2, 2014, pp. 87-97, ISSN 0957-4158.
- [9] M. H. Korayem, M. Yousefzadeh, and B. Beyranvand, Dynamics and Control of a 6-DOF Cable-driven Parallel Robot with Visco-elastic Cables in Presence of Measurement Noise, J Intell Robot Syst 88, 2017, pp. 73–95, doi: 10.1007/s10846-017-0546-1.
- [10] S. Abdolshah, and E. S. Barjuei, Linear quadratic optimal controller for cable-driven parallel robots, 2015 Frontiers of Mechanical Engineering, 10, 2015, pp. 344-351. doi: 10.1007/s11465-015-0364-8.
- [11] J. Jang, and T. Bewley, Tension optimization of the 6-DOF cable-driven boat motion simulator, RSAE 2021, Paris, France, May 2021, doi: 10.1145/3475851.3475854.
- [12] Y. He, and J. Han, Control Lyapunov Functions: New Framework for Nonlinear Controller Design, IFAC Proceedings Volumes, Volume 41, Issue 2, 2008, pp. 14138-14143, ISSN 1474-6670, ISBN 9783902661005, https://doi.org/10.3182/20080706-5-KR-1001.02397.
- [13] Y. Wang and S. Boyd, Fast Evaluation of Quadratic Control-Lyapunov Policy, IEEE Transactions on Control Systems Technology, vol. 19, no. 4, July 2011, pp. 939-946, doi: 10.1109/TCST.2010.2056371.
- [14] K. Galloway, K. Sreenath, A. D. Ames and J. W. Grizzle, Torque Saturation in Bipedal Robotic Walking Through Control Lyapunov Function-Based Quadratic Programs, in IEEE Access, vol. 3, 2015, pp. 323-332, doi: 10.1109/ACCESS.2015.2419630.

- [15] T. Bruckmann, L. Mikelsons, T. Brandt, M. Hiller, and D. Schramm, Wire Robots Part I: Kinematics, Analysis & Design, 2008, doi: 10.5772/5365.
- [16] C. B. Pham, S. H. Yeo, and G. Yang, Tension analysis of cable-driven parallel mechanisms, 2005 IEEE/RSJ International Conference on Intelligent Robots and Systems, 2005, pp. 257-262, doi: 10.1109/IROS.2005.1545368.
- [17] J. Begey, L. Cuvillon, M. Lesellier, M. Gouttefarde, and J. Gangloff, Dynamic Control of Parallel Robots Driven by Flexible Cables and Actuated by Position-Controlled Winches, in IEEE Transactions on Robotics, vol. 35, no. 1, Feb 2019, pp. 286-293, doi: 10.1109/TRO.2018.2875415.
- [18] Y. Yang, and J. Lee, Design of a Control Lyapunov Function for Stabilizing Specified States, IFAC Proceedings Volumes. 43, 2010, pp. 529-534, doi: 10.3182/20100705-3-BE-2011.00088.
- [19] Hassan K. Khalil, Nonlinear Control global edition, Pearson, 2015.
- [20] J. Choi, F. Castañeda, C. Tomlin, and K. Sreenath, Reinforcement Learning for Safety-Critical Control under Model Uncertainty, using Control Lyapunov Functions and Control Barrier Functions, 2020, doi: 10.15607/RSS.2020.XVI.088.
- [21] Q. Nguyen, and K. Sreenath, L1 adaptive control for bipedal robots with control Lyapunov function based quadratic programs, 2015 American Control Conference (ACC), 2015, pp. 862-867, doi: 10.1109/ACC.2015.7170842.
- [22] P. Zhao, Y. Pan, C. Mao, N. Tao, N. Hovakimyan, and X. Wang, Adaptive Robust Quadratic Programs using Control Lyapunov and Barrier Functions, 2020 59th IEEE Conference on Decision and Control (CDC), 2020, pp. 3353-3358.
- [23] M. Grant, and S. Boyd, CVX: Matlab software for disciplined convex programming, version 2.0 beta. http://cvxr.com/cvx, September 2013.
- [24] M. Grant, and S. Boyd, Graph implementations for nonsmooth convex programs, Recent Advances in Learning and Control (a tribute to M. Vidyasagar), V. Blondel, S. Boyd, and H. Kimura, editors, 2008, pp. 95-110, Lecture Notes in Control and Information Sciences, Springer.
- [25] B. Lee, V. Saj, and M. Benedict, Machine Learning Vision and Nonlinear Control Approach for Autonomous Ship Landing of Vertical Flight Aircraft, The Vertical Flight Society, 2021.
- [26] J. L. Sanchez-Lopez, J. Pestana, S. Saripalli, and P. Campoy, An Approach Toward Visual Autonomous Ship Board Landing of a VTOL UAV. J. Intell. Robotics Syst. 74, 1–2, April 2014, pp. 113–127, doi: https://doi.org/10.1007/s10846-013-9926-3.